International Journal of Mechanical Engineering and Technology (IJMET)
Volume 9, Issue 9, September 2018, pp. 1393–1401, Article ID: IJMET_09_09_153
Available online at http://www.iaeme.com/ijmet/issues.asp?JType=IJMET&VType=9&IType=9
ISSN Print: 0976-6340 and ISSN Online: 0976-6359

OPTIMIZATION AND SYNTHESIS OF GOLD NANOPARTICLES ON N-TYPE POROUS SILICON SUBSTRATES AS HIGHLY-GAS SENSITIVE

Wail H. Ali
Mechatronic Engineering Department / Technical Engineering College
Middle Technical University, Baghdad / Iraq

Amer B. Dheyab
Ministry of Science and Technology, Baghdad, Iraq

Alwan M. Alwan
School of Applied Science, University of Technology, Baghdad, Iraq

ABSTRACT

In this work, we report enhanced sensitive surface layer of the porous silicon with the gold (Au) nanoparticles synthesized by anodization technique achieved. The enhanced sensitivity is developing using the electroless metal deposition to form a gold nanostructured framework interacting with the nanopore-coated meso-porous surface. The simple dipping process of Psi in gold (HAuCl4) with concentrations of 1mM diluted in (3M) of HF was employed to synthesize AuNPs. Studies were through analyzing of scanning electron microscopy (SEM), Photoluminescence spectroscopy (PL) and current-voltage (I-V) measurement. The results show that the AuNPs sizes taking place the surface morphology of Psi investigation increase sensitivity for NH3 gas.

Key words: Gold Nanoparticles, mesoPsi, SEM, PL, I-V, Morphology, Sensitivity.

Cite this Article: Wail H. Ali, Amer B. Dheyab, Alwan M. Alwan, Optimization and Synthesis of Gold Nanoparticles on N-Type Porous Silicon Substrates as Highly-Gas Sensitive, *International Journal of Mechanical Engineering and Technology* 9(8), 2018, pp. 1393–1401.
http://www.iaeme.com/IJMET/issues.asp?JType=IJMET&VType=9&IType=8

1. INTRODUCTION

Porous silicon (PSi) has involved much care as a promising electronic material as the detection of its efficient visible room temperature photoluminescence (PL) [1]. There are a number of investigations have shown that the electrical and optical characteristics of porous semiconductors may considerably alteration upon the adsorption of molecules onto their

surfaces [2-5]. The photo-electrochemical etching technique is an attractive technique for fabricating PSi and producing optical waveguides. With this technique, layers can be simple and uniformly fabricated over a large area of the silicon substrate. Semiconducting nanowires are currently attracting much attention as promising mechanisms for future nano-electronic devices such as gas sensor [6–8]. Apply for gas sensing with nano-scale materials in care devices, environmental monitoring, and industrial process controller is a significant field due to anticipated high sensitivity resulting from large surface to volume ratio [9]. It was the preparation of a structure of type (Al/SiNWs/p-Si/Al) for carbonic acid gas sensing. SiNWs were made by metal-assisted chemical etching and modified with noble metals (Au and Pt) using the electroless metal deposition process. [10]. this work, we investigated the effects of the form of n-type porous surface morphology with the formation and preparation mechanism of AuNPs by an ion reduction process reaching the optimum condition and controlling the AuNPs. The investigation of metal on Psi layers can improve the sensitivity of the sensor.

2. FABRICATION AND EXPERIMENTAL

Mirror-like mono-crystalline Si substrates of n-type of a resistivity 10 Ωcm and (100) electrical resistivity were used. The porous layer achieved by a photo-electrochemical etching technique. The experimental setup appears in figure (1).

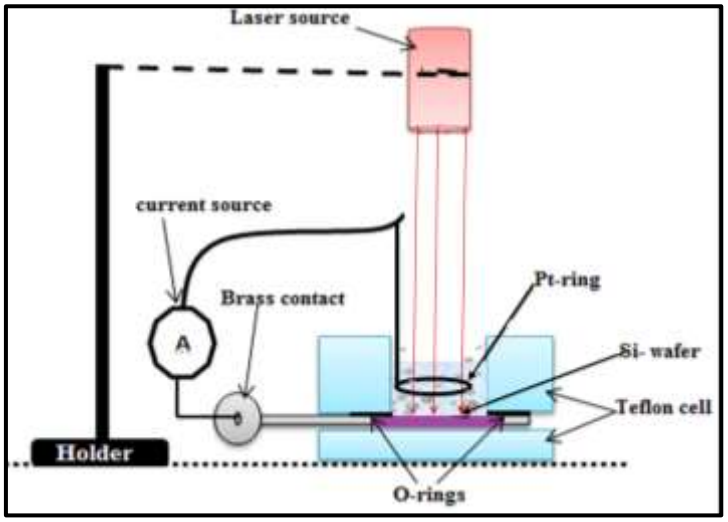

Figure 1 The Experimental setup of a photo-electrochemical etching technique.

The substrates were cutting into rectangles of (2 cm x 2 cm) areas. It anodizations we carried out using a teflon cell with an electrolyte containing 24% HF and ethanol 1:1 by volume. Prepared nanoporous surface prepared under etching conditions of 8 mA /cm^2 for 20 min etching time 18 mW/ cm^2, after anodization, the silicon samples were washed out with deionized water for 10 min and dried under N_2 ambient. Incorporating the porous silicon samples with the Au nanoparticles executed using a dipping process of the surface Psi in the ($HAuCl_4$) solution and high purities 99.98%, (339.7865g/mol) molecular weight and its mixture with HF acid ha been using in this work. Psi samples were dipped in the $HAuCl_4$ solution with concentrations [1mM diluted in (3M) of HF] at the different dipping time using an immersion plating technique. The distributions of AuNPs on the mesoPSi surface achieved by employed scanning electron microscopy (SEM) of type (AIS2300C). The SEM image was analyze with the aid of suitable software image j. The current –voltage characteristics were studies by evaporating an Ohmic contact on the backside of the sample using a thick gold electrode.

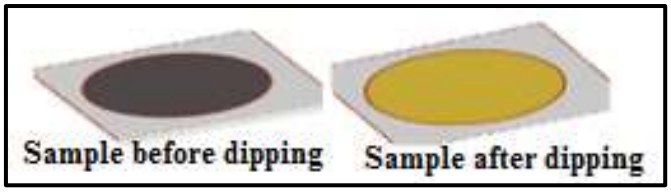

Figure 2 Shows the images of Psi samples before and after dipping prepared by a photo-electrochemical etching technique.

The required volume of the water was calculated based on the following equation [11]:

$$molary = \frac{w(g)}{mW(\frac{g}{mole})} * \frac{1000}{voloum} \quad \ldots\ldots\ldots\ldots\ldots\ldots\ldots \quad (1)$$

Where w: weight, mW: molecular weight,

The dipping process executed in a dark container. AuNPs created naturally as given in the equations [11]:

$$Si + 6HF \longrightarrow H_2SiF_6 + 4H^+ + 4e \qquad E^0 = -1.2V$$

$$Au^{3+} + 3e^- \longrightarrow Au \qquad E^0 = 1.52V$$

Where: large surface area and high porosity lead to high efficiency of gold reduction. The Specific surface area **(S.S.A.)** is a new feature of the material. Metal nanoparticles possess high values of S.S.A. That can calculate via the equation:

$$S.S.A. = \frac{6000}{D * \rho} \quad \ldots\ldots\ldots\ldots\ldots (2)$$

Where: $\boldsymbol{\rho}$: is the density of metal nanoparticles (gm. /cm^3).

3. RESULTS AND DISCUSSION

3.1. Structural Characterization

The morphological of Psi samples (pore size and type) examined by SEM. The analysis of SEM images of PSi substrates shows that it contains large pores with a diameter of about (0.05 -1.25) µm. On the surface, small reflect non homogeneities were also observed, with a higher peak of diameter up to (0.65) µm. Such islands would perhaps occur because of etching and the redeposition of elemental silicon, during photo-electrochemical etching of single crystal plates, with the subsequent oxidation of the porous layer in the air (Fig. 3).

It was found that the sample morphology surface becomes rougher after the deposition of Nanometal on the porous layer (Fig. 4a, b, c, d). The surface of the samples containing deposited tin is the closest in appearance to the original pore surface. The samples with AuNPs and cobalt show a surface different to the original substrate. The surface of these samples a number of nano-sized for AuNPs granules (less than 100 nm). In the figure 4a, found that to consist of AuNPs form large pores with dipping (1min). The figure 4b, consist of AuNPs form very large pores and depth with dipping (2min). While in the figure 4c, d consist of AuNPs start form thin film on pores with dipping (3,4) min, were also all observed on the surface of these samples So, it can speak about the specific isolated nature of the deposited composite film layers and the possible penetration of AuNPs into the interior pores. Where illustrates highly agglomerated AuNPs particles that fully cover the silicon surface.

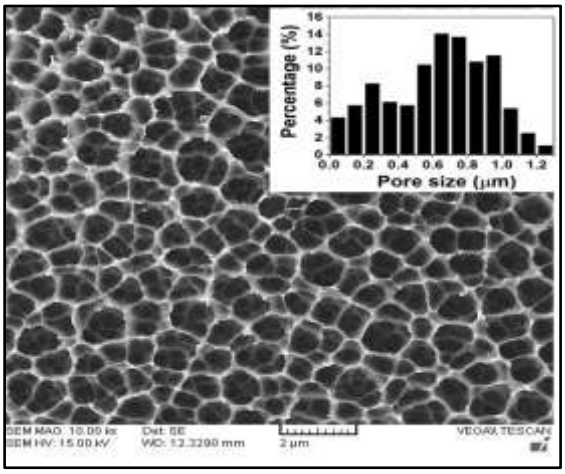

Figure 3 SEM images showing (top view) of as formed mesoPSi with the statistical distribution of pores prepared nanoporous surface prepared at etching time 20 min.

The statistical distribution of particle sizes as a Function of etching time at 20 min with $HAuCl_4$ Concentration 1 mM/3M in figure (4). In the figure 4a, the distribution was varied from (0.025 – 0.575) μm and the peak of the distribution located at (0.025)μm at dipping (1min). In the figure 4b, the distribution was varied from (0.03-0.23)μm and the peak of the distribution located at (0.03)μm at dipping (2min). In the figure 4c, the distribution was varied from (0.035 – 0.155) μm and the peak of the distribution located at (0.035)μm at dipping (3min) and finally the distribution was varied from (0.03 – 0.27) μm and the peak of the distribution located at (0.03)μm at dipping (4min).

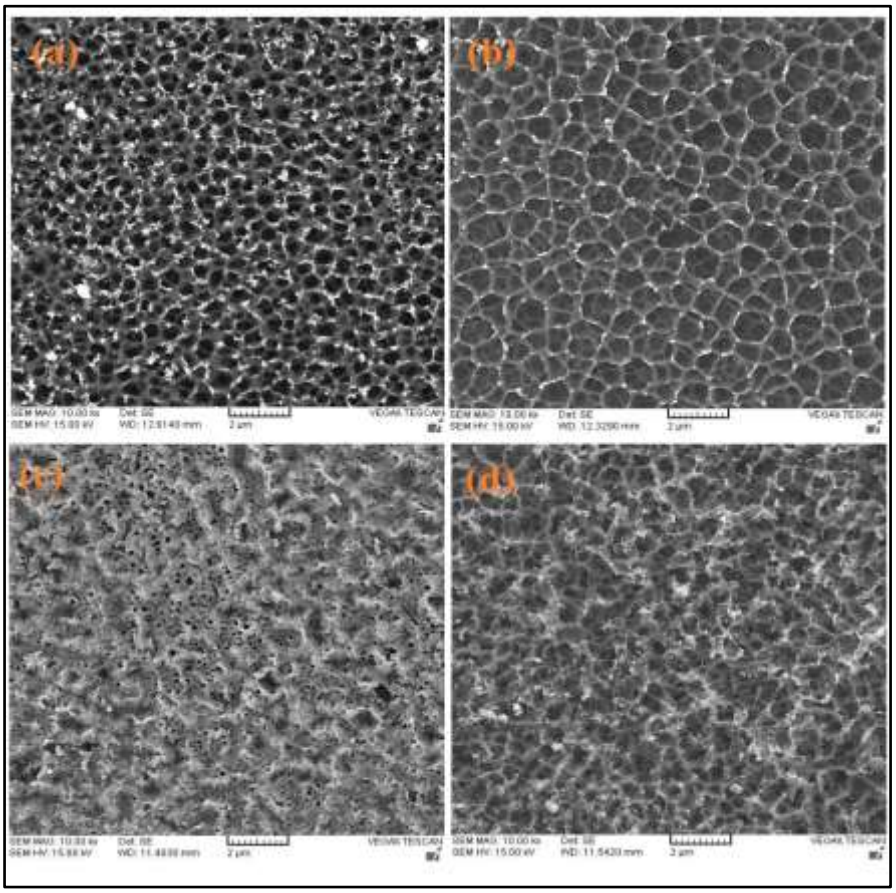

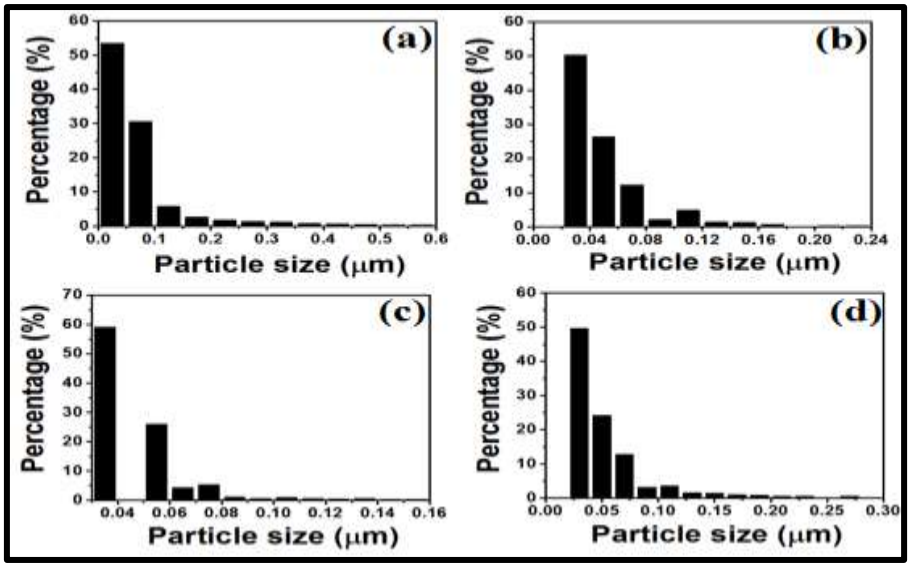

Figure 4 SEM images of gold layer deposited on porous silicon from $HAuCl_4$ (1m M)/3Mm HF the solution at different dipping times a)1 min (b)2 min (c) 3 min (d)4 min with the statistical distribution of particle size.

As we can see from the figure (5a), this increasing of PL intensity accompanied with blue shift is mainly due to quantum size effects in nanostructured Si region, where the blueshift in PL peak is due to the presence of small Si nano size with etching time 20min.

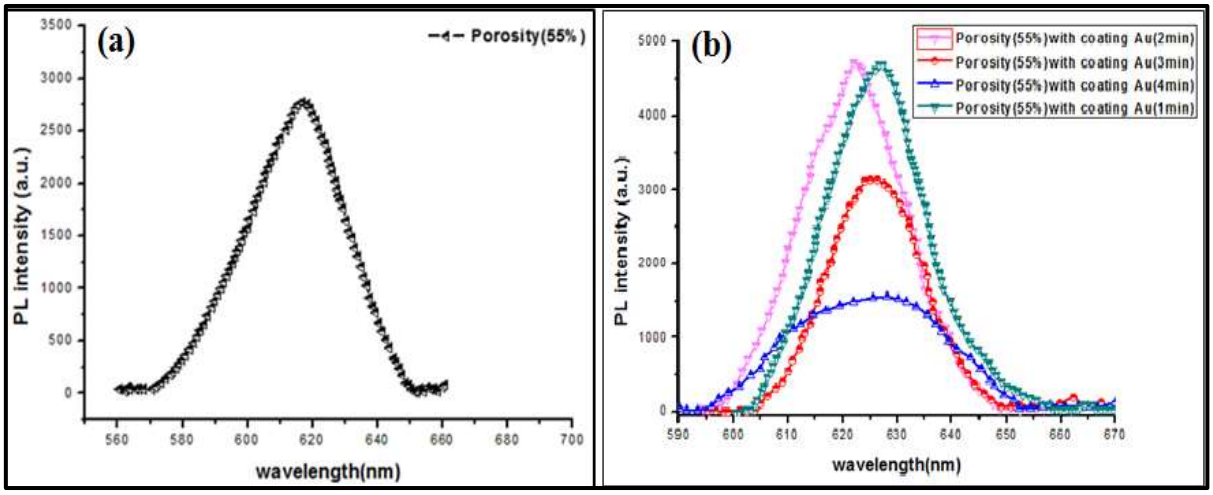

Figure 5 Shows the PL spectra of a) as formed mesoPSi b) AuNPs/PS deposited at C= $5x10^{-3}$ M diluted in HF

The PL spectra, it were quenched in the figure (5a) to the value of (2773a.u.). Then sample deposited at the $HAuCl_4$ (1mM diluted in 3 M of HF). The enhanced to the value of (4687a.u.) at bare porous silicon and observed in the figure (5b) the samples deposited with an $HAuCl_4$ solution with concentration (1mM M diluted in 3 M of HF). It was the enhanced to the value of (4716.31, 3138.3 and 88.6525a.u.) at different dipping time. The PL wavelength, PL peak intensity, PS energy gap, average Si nano-size and hybrid structure AuNPs/Psi are presented in table tabulated in the table (1).Si nano size was calculated using equation (3).

$$E_{g(Psi)=}Eg_{(S)+}88.34/L^{1.37} \quad (3)$$

Where Eg*(eV) is the energy gap of Psi layer, Eg (eV) is the energy gap of bulk silicon and L(A°) is the nano-crystallite size.

Table 1 Shows the values of PL wavelength and PL peak intensity for bare PS samples and hybrid structure AuNPs/PS at a concentration of AuNPs.

Porosity (%)	**PL wavelength(nm)**	**PL peak intensity (a.u)**	**PS energy gap(ev)**	**Si nano size(nm)**
55	617	2773	1.85	3.3

AuNPs concentration(M)	different dipping times(min)	PL wavelength (nm)	PL peak intensity (a.u.)
1mM +3HF	1	627	4687
	2	621.897	4716.31
	3	624.984	3138.3
	4	657.91	88.6525

3.2. Electrical Characterization

The current–voltage (J–V) characteristics of the (Al/mesoPSi/Al) and (Al/AuNPs/mesoPSi/Al) structure, it was analyzed for a 0V to +5V bias voltage. Figs. 6 show the J–V curves of the sensor at a 1mbar pressure in NH_3. The bare porous silicon substrates without of incorporation of AuNPs the characteristics exhibit a linear relationship as in Figs. 6, we observed, under (5) V forward polarization a variation of the current up to (244μm) with gas the prepared device. The forward J–V at AuNPs/mesoPSi substrates without gas exhibit as Schottky relationship as in Figure7.

The forward current –voltage behavior Figure 8 follows as Schottky, where the samples deposited with $HAuCl_4$ solution at dipping time (1 and 2)min was best of at the dipping time (3 and 4) min. The NH_3 adsorption will lead to change in the dielectric constant of the porous layer. The dependence of the dielectric ϵ_{rPsi} on the porosity of the porous layer and the embedding medium ($\epsilon_{r\ pore}$) is given by the equation (3)[12,13].

$$\epsilon_{rPSi} = (1\text{-}P\%)\ \epsilon_{r\ Si}^{1/3} + P\%\epsilon_{r\ pore}^{1/3} \quad (3)$$

Where P % is the porosity of the porous layer, the $\epsilon_{r\ pore}$ is the dielectric constant of the embedding medium NH_3 molecule, the role of dipping time ranging from 1-4min on the I-V characteristics was tested as shown in figure 8. From this figure, we can seen that the increasing of dipping time will improve the conductivity of the AuNPs/mesoPSi sample, but about the best conditions for improving the S.S.A is really related with the minimum AuNPs size that obtain at 2min dipping time. Therefore, the best dipping time is 2min.

The (I-V) characteristics of the sample illuminated porous silicon in the sandwich (Al/AuNPs/mesoPSi/Al) structure configuration mode at different dipping in the absence of NH_3 gas molecules. It was the response of the sensor of the current (S) calculated by the following relation:

$$S = \frac{I_{gas} - I_{air}}{I_{air}} \quad (4)$$

Where Igas and I_{air} characterize the current in the attendance and absent of NH_3 gas respectively

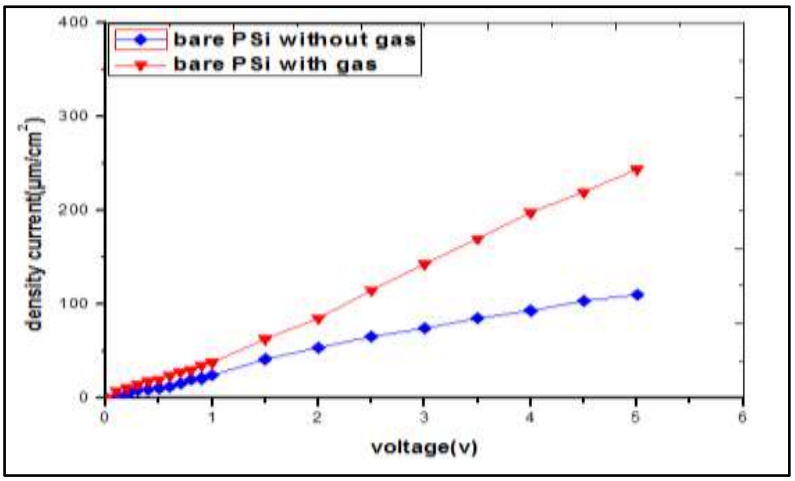

Figure 6 I-V characteristics structure for bare PSi at without gas and with gas at room temperature.

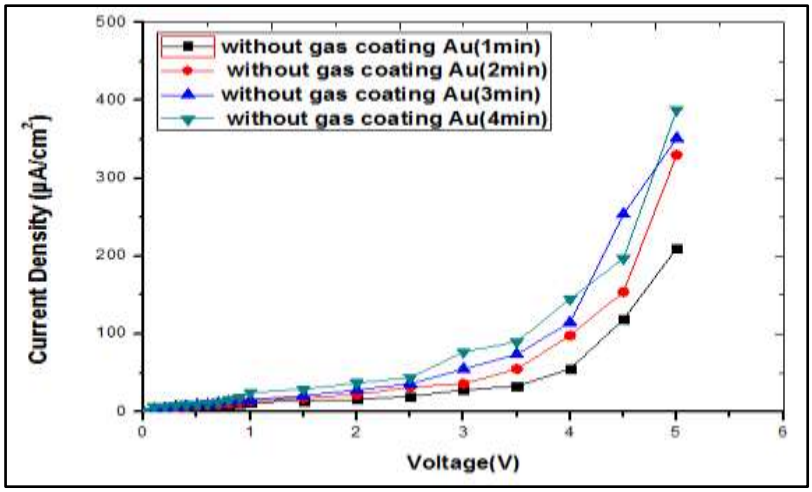

Figure 7 I-V Characteristics structure with different coating gold nanoparticles before NH_3 exposure at room temperature.

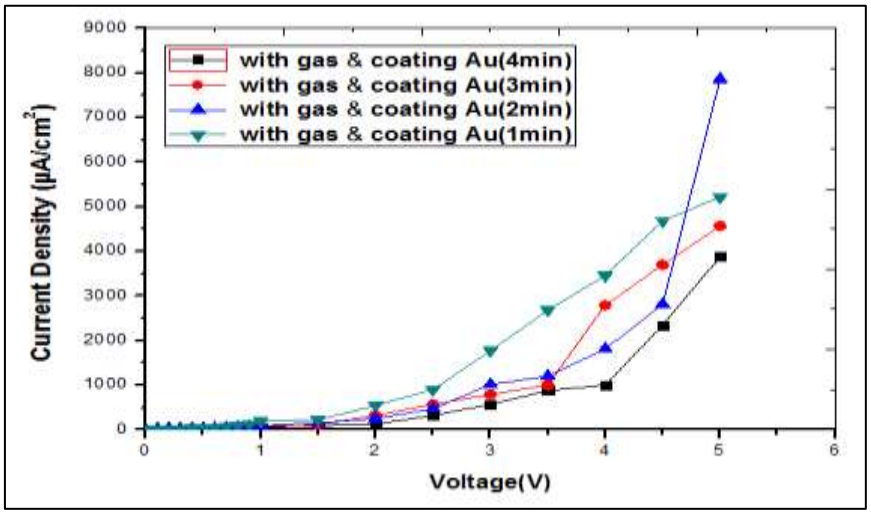

Figure 8 I-V Characteristics of Al/AuNPs/mesoPSi/Al structure with different coating gold nanoparticles after NH_3 exposure at room temperature.

The response of the NH_3 gas of varies the time of the coating gold nanoparticles and coating time used for testing as shown in Figure 9.

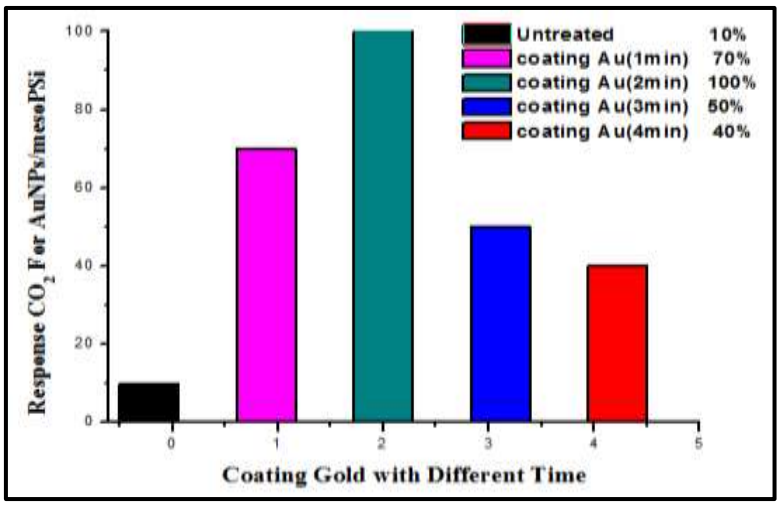

Figure 9 Responses to NH_3 gas from different time coatings on porous silicon.

We can see from the figure (10), the untreated never gives the best response for any of the test gas. The NH_3 gain higher responses with (2 min) gold nanoparticle coating on mesoPSi and there is little change for response in (1 min). The response of NH_3 reduced with increased time (3 and 4) min coating where with passes coated time consist of AuNPs start closed and form a thin film on pores of mesoPSi.

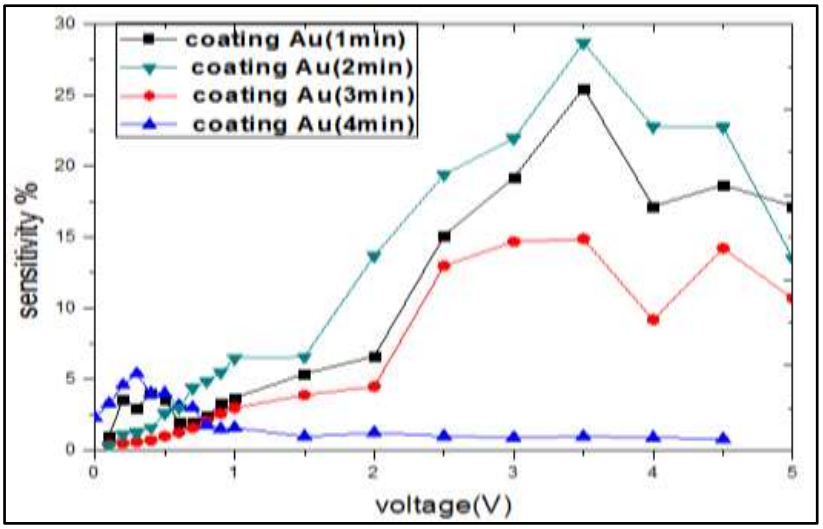

Figure 10 Sensitivity-voltage characteristics of Al/AuNPs/Psi /Al structure with different coating gold nanoparticles after NH_3 exposure at room temperature.

4. CONCLUSIONS

The results presented in this work show that successfully enhanced the sensitivity of porous silicon sensor sensitivity to NH_3 gas. Where gold nanoparticles with mesoPSi lead to high efficiency of sensing when the NH_3 gas interaction with the AuNPs/Psi surface and also It is found that large surface area could be obtained by employing shorter wavelengths and longer irradiation time in the laser-induced etching process. In addition, the developed sensor can operate at voltages in the (1.5) µV range demonstrating a high sensitivity and a low-cost

device with these capabilities may find an important role in automotive, medical, and construction applications. The synthesize hybrid metallic nanoparticles on Psi proves to be an inexpensive and suitability for monitoring environmental pollution levels and gas sensing applications.

COMPLIANCE WITH ETHICAL STANDARDS

This study was funded by School of Applied Science, University of Technology, Baghdad, Iraq and Ministry of Science and Technology, Baghdad, Iraq.

Conflict of interest: The authors declare that they have no conflict of interest**.**

REFERENCES

[1] Charrier J, AlaiwanV, PirastehP, NajarA, GadonnaM, ,(2007) Influence of experimental parameters on physical properties of porous silicon and oxidized porous silicon layers. Appl. Surface Science, 253, 8632- 8636.

[2] L. Canhman, (1997).., Properties of Porous Silicon, INSPEC, London .

[3] Z. C. Feng and R. Tsu, Eds(1994).., Porous Silicon, Word Science, Singapore .

[4] J. J. Mares, J. Kristofik, and E. Hulicius, (1995). "Influence of humidity on transport in porous silicon", Thin Solid Films, 255, 272.

[5] A. G. Cullis, L. T. Canham, and P. D. G. Calcott, (1997)." The structural and luminescence properties of porous silicon", J. Appl. Phys., 82,909 .

[6] J. Goldberger, A. I. Hochbaum, R. Fan, P Yang, (2006)"Silicon Vertically Integrated Nanowire Field Effect Transistors", Nanoletters, 6(5) 973.

[7] C. Yang, C. J. Barrelet, F. Capasso, C.M. Lieber, ,(2006). "Single p-Type/Intrinsic/n-Type Silicon Nanowires as Nanoscale Avalanche Photodetectors, Nanoletters", 6(12) 2929.

[8] Y. Cui, Q. Wei, H. K. Park, C. M. Lieber, (2001)." Nanowire nanosensors for highly sensitive and selective detection of biological and chemical species", Science, 293(5533) 1289,.

[9] A. M. Alwan, R. A. Abbas,(2017),"Effects Of The Porous Silicon Morphology On The Gas Sensor Performance" IJESRT 6(1): January, IC™ Value: 3.

[10] S. Naama a,b,n, T.Hadjersi a,nn, A.Keffous a, G.Nezzal, (2015),"CO2 gas sensor based on silicon nano wires modified with metal nanoparticles" Materials Science in Semiconductor Processing ,01.027i.

[11] A.M. Alwan, I. A. Naseef, (2017) "Optimization of photoluminescence properties of Porous silicon by adding gold nanoparticles"Iraqi Journal of Science, Vol. 58, No.1A, pp: 53-62.

[12] Alwan AM, Dheyab AB (2017) Room temperature CO2 gas sensors of AuNPs/mesoPSi hybrid structures. Appl Nanosci 7:335.

[13] Alwan Mohammed Alwana, Ali Ahmed Yousif b, Layla Alag Wali" The Growth of the Silver Nanoparticles on the Mesoporous Silicon and Macroporous Silicon: a Comparative Study"Indian Journal of Pure & Applied Physics, vol.55,November 2017,pp.813-820.